

Buckling behavior of stainless steel square hollow columns under eccentric loadings

Ho-Ju Jang[†]

Chosun University, 375 Seosuk-dong Dong-gu, Gwangju 501-759, Korea

Seong-Yeon Seo[‡]

Halla University, San 66, Heungup-myon, Wonju-shi, Kangwon-do, Korea

Young-Sung Yang^{‡†}

Chosun University, 375 Seosuk-dong Dong-gu, Gwangju 501-759, Korea

(Received March 15, 2005, Accepted April 3, 2006)

Abstract. This study involves a series of experiments on the buckling strength of eccentrically compressed cold-formed stainless steel square hollow-section columns. The principal parameters in this study are slenderness ratios ($L_k/r = 30, 50, 70$) and magnitude of eccentricity e (0, 25, 50, 75, 100 mm) on the symmetrical end-moment. The objectives of this paper are to obtain the buckling loads by conducting a series of experiments and to compare the behavior of the eccentrically compressed cold-formed stainless steel square hollow-section columns with the results of the analysis. The ultimate buckling strength of the square-section members were determined with the use of a numerical method in accordance with the bending moment-axial force (M - P) interaction curves. The behavior of each specimen was displayed in the form of a moment-radian (M - θ) relationship. The numerically obtained ultimate-buckling interaction curves of the beam columns coincided with the results of the experiments.

Keywords: stainless steel; square hollow sections; axial force; symmetrical end-moment; slenderness ratio; magnitude of eccentricity; moment-axial force (M - P) interaction curves.

1. Introduction

Column members should absorb the energy from vertical and horizontal loads. For this to happen, however, the column members' strength should not be reduced suddenly due to local buckling until the said strength reaches its maximum from the yield strength (Bleich 1952, Chen and Atsuta 1976, Johnson *et al.* 1996).

Furthermore, most columns receive moments from their vertical or horizontal load due to

[†] Doctor

[‡] Associate Professor, Corresponding author, E-mail: 95148@halla.ac.kr

^{‡†} Professor

eccentricity, and as compressive power occurs with respect to the sinking column also due to the moment, the geometrical moment of inertia occurs due to the composition of the flexural and compressive forces. This feature of columns can be understood by conducting beam column experiments, in which the columns receive moments by eccentricity.

As stainless steel has superior durability and plastic deformation ability, it is judged that it can be used as a structural member (Japan Stainless Steel Association 1995). Therefore, it is proposed that modification of existing standards is required through experiments and analysis to utilize stainless steel's structurally superior characteristics. Many studies have been conducted on this subject, but with respect to general structural steel columns. This study, however, aims to determine the effects of the vertical load, by eccentricity, on the square hollow section of a stainless steel column so as to ascertain the adaptability of stainless steel columns as structural materials. It also aims to find out the mechanical character of a stainless steel square hollow column, including its maximum strength and transformation ability, among others, using its slenderness ratio with its symmetrical end-moment and eccentric ratio (e/k), among others, as major variables. By comparing these characteristics with the experimental values through theoretical analysis, this study seeks to gather basic data to establish standards for the structural design of stainless steel columns.

2. Test plan

The stainless steel square hollow section used in this study was \square -100 \times 100 \times 3.0, STS 304 TKC in the austenite line, manufactured by KS D 3536 (stainless steel for machinery structures). Its F_y was defined as 205 N/mm².

2.1 Coupon test and stub-column test

To understand the mechanical character of the materials used in this study, a coupon test was conducted on the tensile-strength test piece, from which the residual stress was almost completely removed, by sampling three test pieces from the flat-board part of the test piece. The test pieces were patterned after the No. 5 test piece (stainless steel section) defined in KS B 0801 (test piece for the tensile test of metal materials), and the test was performed using KS 0802 (the coupon test method for metal materials).

The stub-column test had almost no effect on the slenderness ratio and was designed to determine the local buckling strength and the yield stress of the pure compressive force of the stainless steel section, including the residual stress. In this test, three test particles were prepared, each with a width three times that of the actual stainless steel section, based on the standards of the SSRC (Structural Stability Research Council) of the U.S. for the short-column test, which is the appropriate length of the test particle with no effect on the slenderness ratio (i.e., the length can be reduced without producing the flexural buckling effect).

Table 1 shows the values measured from the test particles as a cross-sectional function of the stub-column test particles.

By making the end-constraint condition of the test particle simply support its status, the impact of eccentricity is minimized; and by establishing a spherical block in the lower part of the test particle, with equally distributed loads, through central compression, it is simply loaded as U.T.M.

Table 1 Sectional function of the stub-column test particles

Classification	B (mm)	t (mm)	A (cm ²)	L (mm)	I (cm ⁴)	r (mm)	S (cm ³)	Z (cm ³)	f
Stub-column	101.4	2.82	11.13	299.8	180.53	40.3	35.60	42.78	1.17

Note: B = width; t = thickness; A = sectional area; L = length; I = sectional geometrical moment of inertia; r = sectional diameter of inertia; S = sectional elastic modulus; Z = sectional plastic modulus; and f = shape factor.

For the measurement method, a wire strain gauge (hereinafter referred to as “W.S.G.”) was placed in the middle part of the test particle to measure the wire strain of the test particle. To measure the general axial displacement, a displacement transducer was established (hereinafter referred to as “D.T.”).

2.2 Eccentric compression column test

For columns that receive axial force and moment at the same time, equal eccentric axial loads are regarded as effective. Thus, the test for the eccentrically compressed columns was conducted in this study, assuming the status of the actual column’s strength. For the test particles, a total of 15 columns were produced, which were buckled in the inelastic region with slenderness ratios (KL/r) of 30, 50, and 70, and which received symmetrical end-moments with eccentric ratios (e/k) of 0, 1.5, 3.0, 4.5, and 6.0 upon each slenderness ratio, respectively.

Table 2 shows the plan for the test particles (values of the test particles by actual measurement), and Fig. 1 shows the degree of force applied to the test particles.

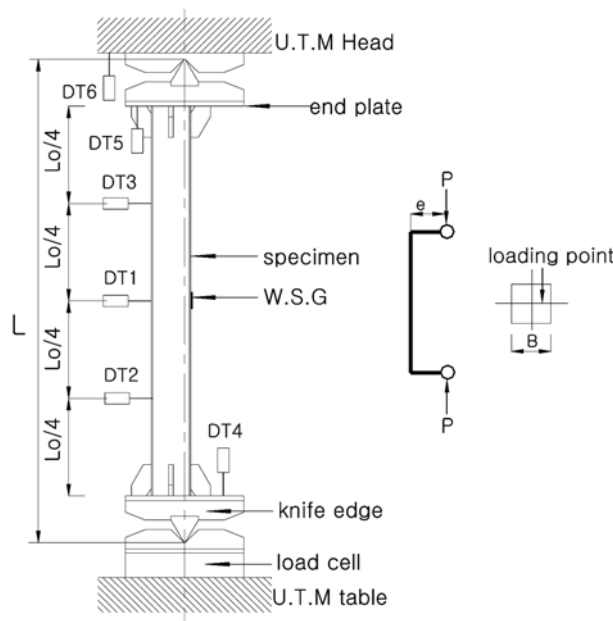


Fig. 1 Picture of load on the column test particles

Table 2 Plan of the test particles

Name of the particles	k (mm)	L_k/r	L_0 (mm)	e (mm)	e/k	L (mm)	K	L_k (mm)
C-30-0				0	0	1186	0.981	1163
C-30-25				25	1.5	1193	0.957	1142
C-30-50	16.60	30	959	50	3.0	1193	0.957	1142
C-30-75				75	4.5	1193	0.957	1142
C-30-100				100	6.0	1193	0.957	1142
C-50-0				0	0	1981	0.993	1968
C-50-25				25	1.5	1979	0.983	1945
C-50-50	16.60	50	1745	50	3.0	1979	0.983	1945
C-50-75				75	4.5	1979	0.983	1945
C-50-100				100	6.0	1979	0.983	1945
C-70-0				0	0	2772	0.997	2763
C-70-25				25	1.5	2778	0.991	2753
C-70-50	16.60	70	2544	50	3.0	2778	0.991	2753
C-70-75				75	4.5	2778	0.991	2753
C-70-100				100	6.0	2778	0.991	2753

Note: k = sectional-core diameter; L_0 = pure length of the test particle; e = magnitude of eccentricity; e/k = eccentric ratio; L = buckling length (L_0 + endplate (9 mm, 12 mm) \times 2 + knife edge (105 mm) \times 2); K : effective buckling length coefficient, L_k : effective buckling length ($L \times K$)

In the forcing method, the test particles were loaded under the symmetric simple-support condition, with a maximum capacity of 1000-kN U.T.M. To achieve symmetry of the test particles, the edge of a knife was used, which could be rotated in only one direction and which minimized the end-constraint. Here, it calculated the equal buckling length (L_k) considering the endplates attached at both ends, and the effects of the ridged zone caused by the edge of the knife. For the slenderness ratio, it used the sectional diameter of inertia (r).

In addition, since the test particles, whose eccentric ratio was 0, were hardly affected by the end-moment, they were welded with the 9-mm-thick endplate without a bracket. The test particles with eccentric ratios of over 1.5 were welded with a 12-mm-thick endplate and a bracket onto the center of the four sides, and the edge of the knife and bolt were connected to minimize the strain of the rigid zone that was connected using bolts by the endplate moment.

For the method of measurement, the W.S.G. was attached to the part where the largest strain was anticipated, and the D.T. was established to measure the axial, vertical, and angular displacements, among others.

3. Theoretical analysis

The strength assessment method, through theoretical analysis, was used to assess the strength of the column as it maintained a constant axial force on the steel hollow-section column, and it was assumed that the steel hollow section was subjected to full-plastic stress according to the increase in the load of the moment when the moment was operated.

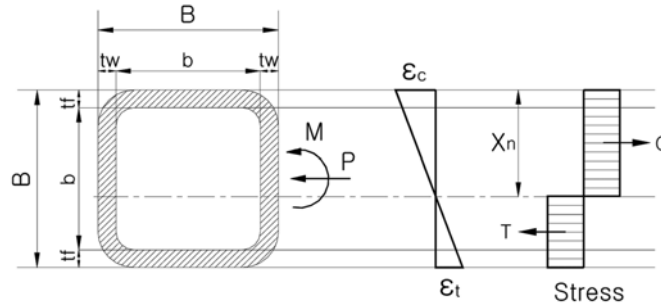


Fig. 2 Full-plastic stress distribution

When the axial force and moment were operated, the full-plastic stress block of the sectional factor of the stainless steel square hollow section shown in Fig. 2 was calculated by leading the M - P interaction from the equilibrium condition of force according to the location of the neutral axis and by considering the P - δ effect based on the changes in the slenderness ratio (moment extension coefficient - A_F) (AISC 2001).

For the evaluation of the maximum strength of the stainless steel square hollow section, the following were assumed:

- 1) The shape of the hollow section was square.
- 2) The stainless steel square hollow section should remain a plane after its strain.
- 3) Under the full-plastic stress condition, the tensile stress and the compressive stress on the section performed rectangular stress distribution.
- 4) For the effects of the sloping of the materials and the eccentric load, the moment expansion coefficient (A_F) and the stress reduction coefficient ($\phi = 0.85$) were applied (SEI/ASCE-8 2003).

The computation of the stress under the full-plasticity condition was divided into the following three ranges, according to the location of the plastic neutral axis (X_n): $0 < X_n < t_f$; $t_f \leq X_n < t_f + b$; and $t_f + b \leq X_n < B$.

In Fig. 2, if the neutral axis is assumed to be within the range of $t_f \leq X_n < t_f + b$, the compressive force and the tensile force under the full-plasticity status would be as follows:

$$C = [B \times t_f + 2(X_n - t_f) \times t_w] \times \sigma_y; \text{ and}$$

$$T = [B \times t_f + 2(B - X_n - t_f) \times t_w] \times \sigma_y$$

The moment of the compressed side (M_C) in the section and the moment of the tensile side (M_T) are as follows, from the resultant force of stress and the neutral axis in the section:

$$M_C = (t_f \times B \times \sigma_y) \times \left(X_n - \frac{t_f}{2}\right) + [2 \times t_w \times (X_n - t_f) \times \sigma_y] \times \left(\frac{X_n - t_f}{2}\right); \text{ and}$$

$$M_T = (t_f \times B \times \sigma_y) \times \left(B - X_n - \frac{t_f}{2}\right) + [2 \times t_w \times (t_f + b - X_n) \times \sigma_y] \times \left(\frac{t_f + b - X_n}{2}\right)$$

The axial force (P) and the moment (M_{PCO}), which were operated in the section under the full-

plastic stress status, were calculated as follows from the equilibrium conditions of the axial directional force (C , T) and the moment (M_C , M_T) in the section:

$$P = C - T; \text{ and}$$

$$M_{PCO} = M_C + M_T - P \times \left[(t_f - X_n) + \frac{b}{2} \right]$$

The axial force (P_{PC}), considering the slenderness effect based on the changes in the slenderness ratio, and the moment, were calculated as follows, considering the maximum strength (P , M_{PCO}), the buckling coefficient (α), and the moment expansion coefficient (A_F):

$$P_{PC} = P \times \alpha; \text{ and}$$

$$M_{PC} = M_{PCO} \times \frac{1}{A_F} = M_{PCO} \times \left(1 - \frac{P}{\phi \times P_e} \right)$$

where $\alpha =$ the buckling coefficient considering the slenderness ratio ($0.658^{\lambda_c^2}$);

$\lambda_c =$ the dimensionless slenderness ratio $\left(\frac{KL}{r\pi} \times \sqrt{\frac{\sigma_y}{E}} \right)$; and

$P_e =$ the Euler buckling load $\left(\frac{\pi^2 EI}{L_k^2} \right)$; $\phi =$ the strength reduction factor.

$E =$ the stainless steel tangent modulus

Fig. 3 is the M - P interaction curve of the stainless steel square hollow section, computed through theoretical analysis (Chen and Atsuta 1976). In the theoretical equation, the yield axial force (P_y), which was the 0.1% offset stress of the stub-column, and the full-plastic moment (M_p), which was calculated using the plastic section coefficient (S) actually measured by the stub-column, were applied.

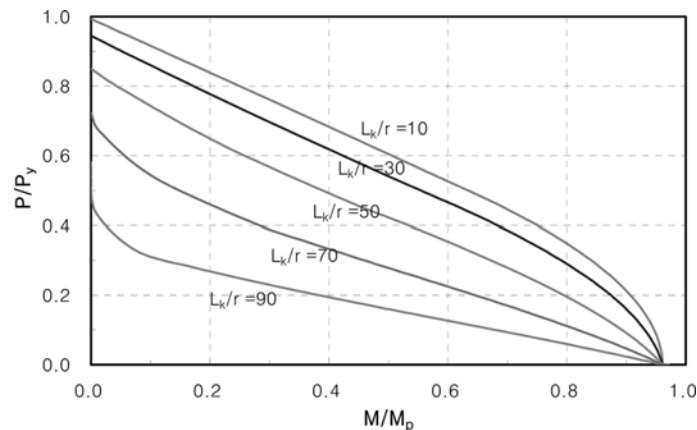


Fig. 3 M - P interaction curve computed through theoretical analysis

Table 3 Coupon and stub-column test results

Classification	σ_{\max} (N/mm ²)	ϵ_{\max}	0.1% offset				0.2% offset				S (%)	ϵ (%)
			σ_y (N/mm ²)	σ_y/σ_{\max}	ϵ_y	${}_s\sigma_y/{}_t\sigma_y$	σ_y (N/mm ²)	σ_y/σ_{\max}	ϵ_y	${}_s\sigma_y/{}_t\sigma_y$		
Coupon	1	833	0.5252	388	0.47	0.0025	415	0.50	0.0036	45.68	50.10	
	2	822	0.5353	387	0.47	0.0024	427	0.52	0.0035	46.90	50.20	
	3	838	0.4525	382	0.46	0.0028	418	0.50	0.0040	44.99	52.70	
	Ave.	831	0.5044	386	0.46	0.0026	420	0.51	0.0037	45.86	51.00	
Stub-column	1	409	0.0052	317	0.78	0.0024	0.82	386	0.95	0.0037	0.93	
	2	410	0.0051	340	0.85	0.0031	0.88	399	0.97	0.0044	0.93	
	3	400	0.0053	318	0.79	0.0027	0.83	381	0.95	0.0040	0.91	
	Ave.	406	0.0052	327	0.81	0.0027	0.85	389	0.96	0.0040	0.93	

Note: σ_{\max} = maximum (tensile) stress; ϵ_{\max} = strain intensity at the maximum stress; σ_y = yield stress; σ_y/σ_{\max} = yield ratio; ϵ_y = strain intensity at the yield ratio; ${}_s\sigma_y$ = yield stress of the stub-column; ${}_t\sigma_y$ = yield stress of the tensile-strength test particle; S = sectional contraction ratio; and ϵ = elongation ratio.

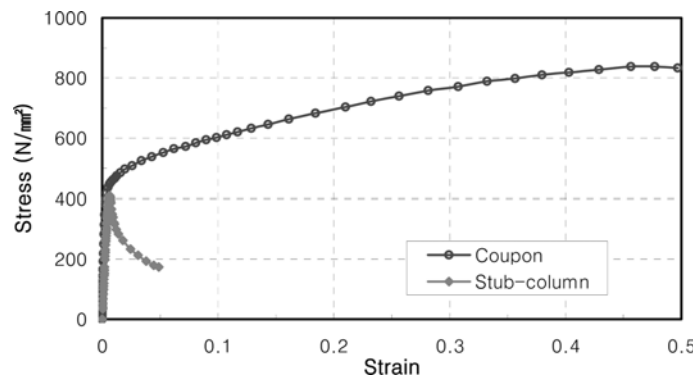


Fig. 4 Stress-strain intensity curve

4. Test results

4.1 Coupon and stub-column test results

Table 3 shows the maximum stress (σ_{\max}), yield stress (σ_y), yield ratio (σ_y/σ_{\max}), and elongation ratio (ϵ) from the coupon and stub-column test results. Fig. 4 on the other hand, describes the unit stress and the stain intensity. Based on the results of the coupon, the yield plateau did not appear in the test piece, and since the stress of the stainless steel square hollow section increased after the yield, it showed a very high tensile stress value of over 800 N/mm², and the stain intensity in the maximum stress showed a value of 0.5 ($\times 10^6$ strain).

As a result of the tensile stress test conducted on steel, if the yield point does not appear, the KS standards prescribes the use of 0.2% offset stress, and Japan uses 0.1% offset stress according to its “Design Standards and the Explanations of the Stainless Steel Structural Engineering Association”. Therefore, this study presented the yield stress as 0.1% offset stress and 0.2% offset stress.

Comparing each yield stress of the stainless steel square hollow sections with the yield standard stress of the stainless steel square hollow section regulated in the KS, it was found that the average yield stress of the stainless steel square hollow section, calculated by the 0.1% offset stress, was 386 N/mm², which was 1.88 times higher than the standard stress; and the yield stress, calculated by the 0.2% offset stress, was 420 N/mm², which was two times higher than the standard stress. The elongation ratio was 51%, which indicates very high elongation ability.

The average maximum stress from the stub-column test was 406 N/mm², and the strain intensity at the maximum stress was 0.0052. The 0.1% offset average yield stress was 327 N/mm², the yield ratio was 0.81, the 2% offset yield stress was 389 N/mm², and the yield ratio was 0.93.

The yield stress of the stub-column and the yield stress from the tensile-strength test were 0.85 and 0.93, respectively. This is regarded as the impact of the plastic processing or residual stress.

Fig. 4 shows the unit stress-strain intensity curve of the tensile-strength test piece and the stub-column.

As shown in Fig. 4, the curve of the coupon test piece shows a constant increase of stress up to the maximum stress from the yield stress, as well as superior strain ability. However, the stub-column curve showed a sudden stress reduction from local buckling after the maximum stress, since it showed a slight plastic strain throughout the yield stress.

4.2 Eccentrically compressed column test

The buckling stress of the eccentrically compressed column is defined based on the buckling load of the column obtained through the test. The maximum stress, the local buckling stress, the

Table 4 Eccentrically compressed column test results

Name of the test particles	e/k	σ_{\max} (N/mm ²)	σ_{loc} (N/mm ²)	M (kN·m)	$\sigma_{\max}/s\sigma_{\max}$	$\sigma_{\max}/s\sigma_y$	M/M_p
C-30-0	0	393	385	0	0.97	1.20	0
C-30-25	1.5	244	240	6.80	0.60	0.75	0.49
C-30-50	3.0	186	183	10.35	0.46	0.57	0.71
C-30-75	4.5	143	142	11.94	0.35	0.44	0.85
C-30-100	6.0	112	111	12.41	0.28	0.34	0.89
C-50-0	0	347	318	0	0.85	1.06	0
C-50-25	1.5	197	195	5.48	0.49	0.60	0.39
C-50-50	3.0	153	150	8.53	0.38	0.47	0.61
C-50-75	4.5	122	120	10.20	0.30	0.37	0.73
C-50-100	6.0	102	100	11.38	0.25	0.31	0.81
C-70-0	0	217	175	0	0.53	0.66	0
C-70-25	1.5	143	131	4.01	0.36	0.44	0.29
C-70-50	3.0	112	109	6.23	0.28	0.34	0.45
C-70-75	4.5	91	88	7.56	0.22	0.28	0.54
C-70-100	6.0	79	76	8.82	0.19	0.24	0.63

Note: σ_{\max} = maximum stress; σ_{loc} = local buckling stress; M = moment calculated by the magnitude of eccentricity and the buckling stress; $s\sigma_y$ = average yield stress of the stub-column calculated using the 0.1% offset method; and M_p = full-plastic moment ($M_p = Z \cdot \sigma_y$).

eccentricity, the moment calculated by the eccentric load, the ratio of the maximum stress, and others, of each test particle are described in Table 4.

4.2.1 Maximum stress and local buckling stress

The maximum stress was calculated from the maximum load that the column could support, and all the experimental particles were chosen according to the member buckling. With respect to the test results, the test particle with a slenderness ratio of 30 and an eccentric ratio of 0 showed the largest maximum stress (393 N/mm²), and the test particle with a slenderness ratio of 70 and an eccentric ratio of 6.0 showed the smallest maximum stress (79 N/mm²). The test results show that the maximum stress of the eccentrically compressed column was clearly reduced when the slenderness ratio and the eccentric ratio increased.

Fig. 5 shows the maximum stress according to the changes in the eccentric ratio produced by each slenderness ratio. All the test particles of the slenderness ratio showed a drastic reduction of stress in the initial period as the eccentric ratio increased, and later showed a slow reduction. Compared to the test particles with an eccentric ratio of 30, the test particles with an eccentric ratio of 50 showed 80.74-91.07% stress values, and the test particles with an eccentric ratio of 70 showed 55.22-70.54% stress values. As seen in these values, the reduction ratio decreased with the increase in eccentric ratio.

Fig. 6 shows the comparative curve of the maximum stress of each eccentric ratio based on the changes in the slenderness ratio. For all eccentric ratios, as the slenderness ratio increased, the stress decreased; and as the eccentric ratio increased, the maximum stress decreased. However, the reduction of stress based on the increase in the eccentric ratio became slower. This is attributed to the effect of the flexure, rather than of the compressive force, on the maximum stress of the column based on the increase in the eccentric ratio.

Moreover, when the maximum buckling stress of the column was compared with the maximum stress of the short column or the 0.1% offset yield stress—i.e., 0.97-0.19 and 1.20-0.24, respectively—it was found that the maximum buckling stress of the column showed a bigger stress reduction phenomenon when the slenderness ratio and the eccentric ratio increased.

Since the local buckling stress was calculated from the point when drastic stress reduction started

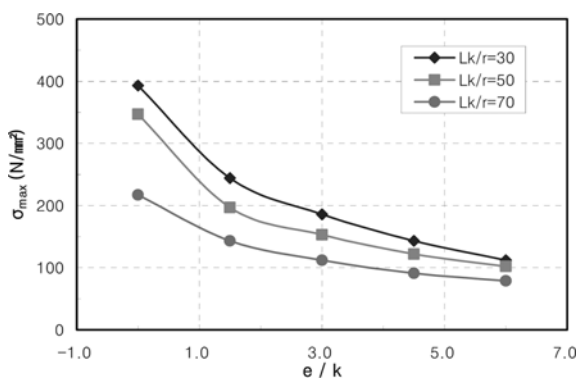


Fig. 5 Maximum stress based on the changes in the eccentric ratio

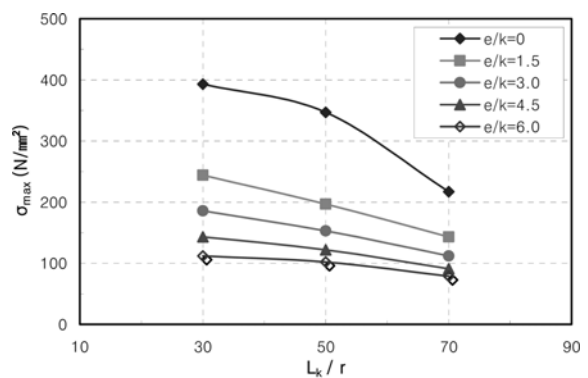


Fig. 6 Maximum stress based on the changes in the slenderness ratio

from the maximum stress in the unit stress-strain intensity curve of the test results, it could be uncertain.

The local buckling occurred, however, after the maximum stress was reached in all the test particles. The local buckling stress of the column showed a maximum value of 385 N/mm^2 in the C-30-0 test particle, and the C-70-10.0 test particle showed the lowest maximum stress (76 N/mm^2). Consequently, the average of the maximum buckling stress was 96.04%, but the test particles with an endplate moment in the magnitude of eccentricity, excluding the test particles with an eccentric ratio of 0 and that which received central compression, showed a maximum stress of 97.53%, with almost no deviation in the results.

4.2.2 Relationship of buckling stress with displacement

The buckling stress-displacement curve of the test particles of the column was described in Figs. 7 and 8, according to their eccentric ratios, respectively. The vertical axes in the figures represent the buckling stress, and the horizontal axes made the vertical displacement (Δ) and the horizontal displacement (δ) dimensionless through the effective buckling length (L_K) of the column.

As seen in Fig. 7, as the eccentric ratios based on each slenderness ratio increased, the buckling stress decreased and the axial displacement largely increased.

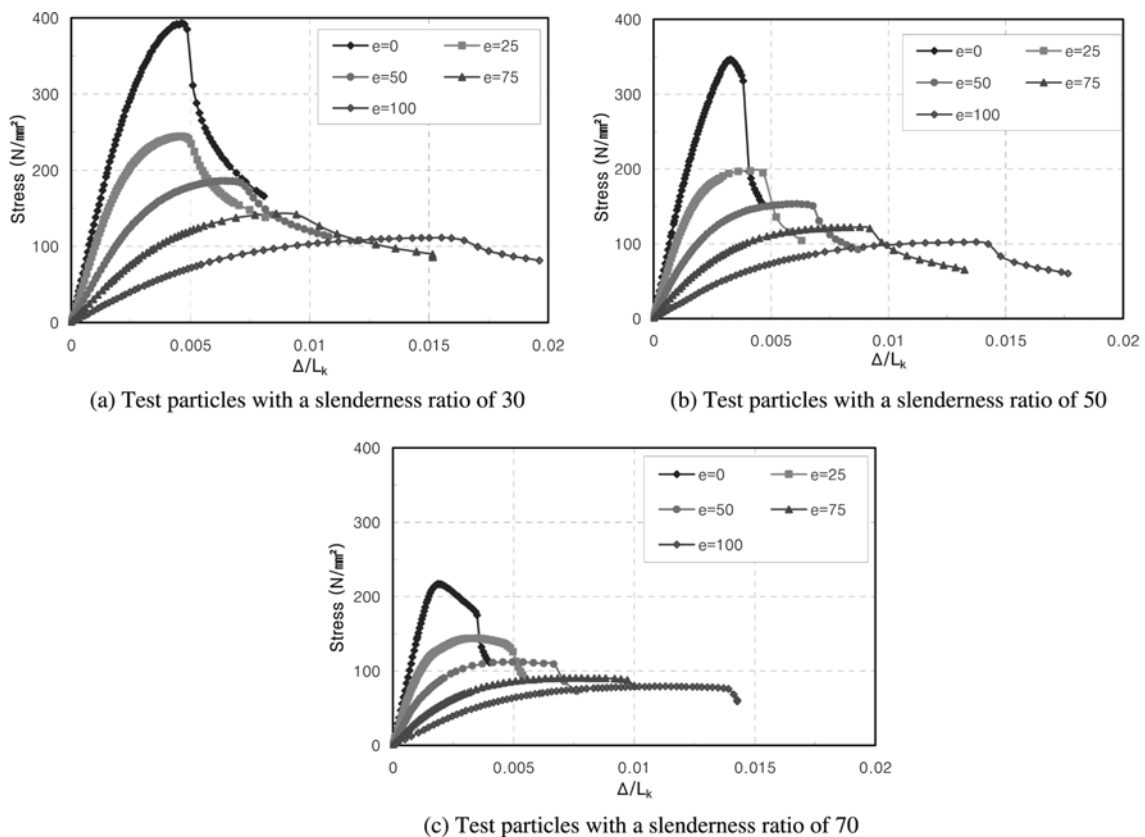


Fig. 7 Buckling stress-axial displacement curves

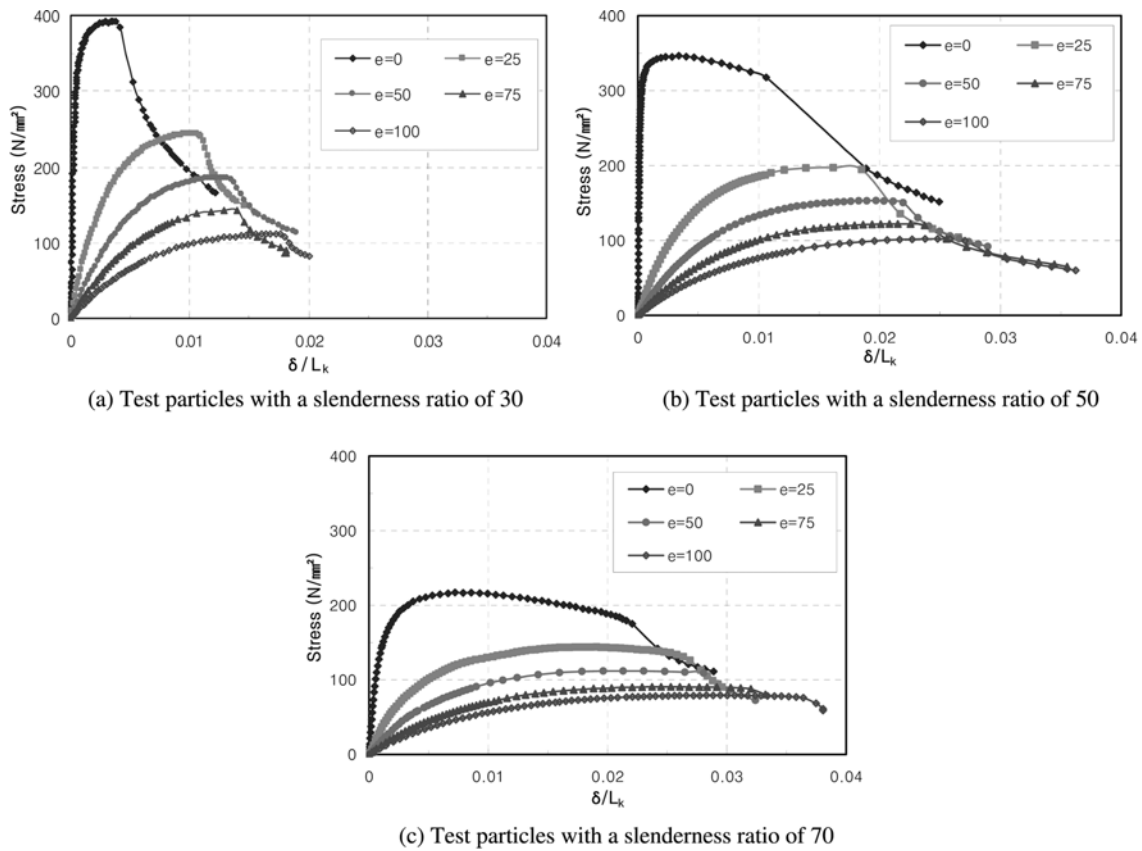


Fig. 8 Buckling stress-horizontal displacement curves

Moreover, based on the increase in the slenderness ratio, the axial displacement gradually decreased and the width of the axial displacement on the maximum stress dropped by 88.92% on the average in the test particles with a slenderness ratio of 50, and by 70.30% on the average in the test particles with a slenderness ratio of 70, compared to the test particles with a slenderness ratio of 30.

In Fig. 8, the horizontal displacement (unlike the axial displacement) increased as the slenderness ratio increased, and the eccentric ratio increased in each slenderness ratio. According to the increase in the slenderness ratio, the width of the horizontal displacements also increased to 147% in the test particle with a slenderness ratio of 50, and to 188% in the test particle with a slenderness ratio of 70, on the average, based on the test particle with a slenderness ratio of 30.

Comparing the buckling stress with the displacement of the eccentrically compressed column, as the slenderness ratio increased, it was affected more by the flexure than by the compressive force, so that the buckling stress due to the member buckling of the stainless steel square hollow section and the axial displacement decreased, and the vertical displacement seemed to increase with the slenderness effect and the endplate moment due to the increase in the eccentric ratio.

4.2.3 Relationship of the moment with the rotation angle

To determine the moment and the strain of the test particles of the eccentric column according to the slenderness ratio, the relationship between moment, which became dimensionless at the full-

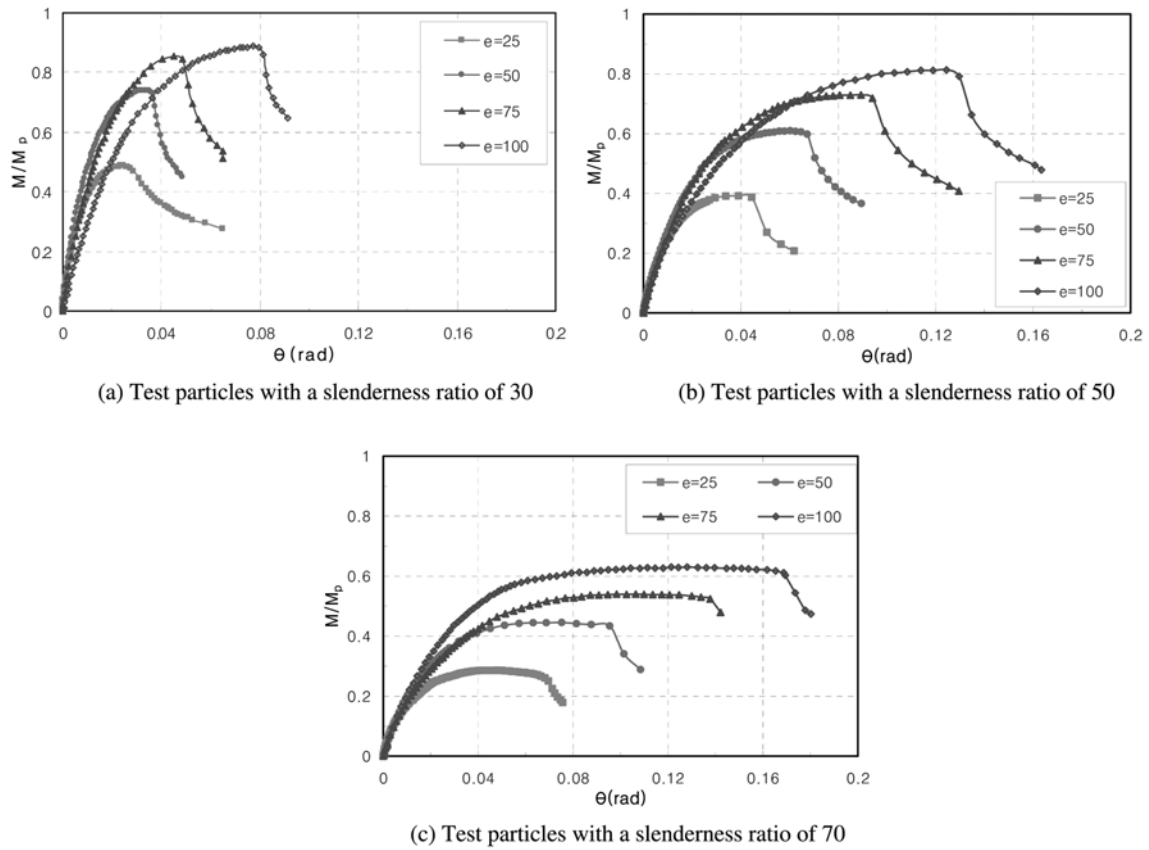


Fig. 9 Moment-rotation angle curves

plastic moment based on the eccentric ratio, and the endplate rotation angle (θ) of the test particles is described in Fig. 9.

As shown in Fig. 9, the moment and rotation angles increased according to the increase in the eccentric ratio in all the test particles for each slenderness ratio. Since their rates of increase were almost the same, the maximum moment turned out to be 1.54 times the average value and the rotation angle, 1.48 times the average value in the eccentric ratio of 3.0; 1.83 and 2.01 times, respectively, in the eccentric ratio of 4.5; and 2.03 and 2.96 times, respectively, in the eccentric ratio of 5.0, compared to those in the eccentric ratio of 1.5.

For the increase in the slenderness ratio, however, the moment decreased but the rotation angle increased. Compared to the maximum moment and rotation angle of the test particle with a slenderness ratio of 3.0, the moment decreased to 0.81, 0.82, 0.85, and 0.91, and the rotation angle increased to 1.57, 1.82, 1.89, and 1.62 in the test particle with a slenderness ratio of 50; and the moment decreased to 0.59, 0.60, 0.64, and 0.71, and the rotation angle increased to 1.94, 2.27, 2.18, and 1.62 in the test particle with a slenderness ratio of 70. It was found that the buckling of the eccentric column was largely affected by the increase in the moment of the endplate due to the increase in the eccentric ratio, and by the increase in the rotation angle of the endplate due to the increase in the slenderness ratio.

Table 5 Test results and analysis results of the eccentric column test

Name of the test particles	e/k	Test results (A)		Analytical results (B)		A/B	
		P/P_y	M/M_p	P/P_y	M/M_p	P/P_y	M/M_p
C-30-0	0	1.20	0	0.95	0	1.27	0
C-30-25	1.5	0.75	0.49	0.62	0.40	1.21	1.22
C-30-50	3.0	0.57	0.71	0.47	0.59	1.21	1.20
C-30-75	4.5	0.44	0.85	0.37	0.72	1.18	1.19
C-30-100	6.0	0.34	0.89	0.30	0.79	1.13	1.13
C-50-0	0	1.06	0	0.85	0	1.25	0
C-50-25	1.5	0.60	0.39	0.53	0.34	1.13	1.13
C-50-50	3.0	0.47	0.61	0.41	0.52	1.14	1.18
C-50-75	4.5	0.37	0.73	0.33	0.63	1.11	1.16
C-50-100	6.0	0.31	0.81	0.27	0.71	1.14	1.14
C-70-0	0	0.66	0	0.72	0	0.91	0
C-70-25	1.5	0.44	0.29	0.41	0.27	1.08	1.09
C-70-50	3.0	0.34	0.45	0.33	0.41	1.04	1.10
C-70-75	4.5	0.28	0.54	0.27	0.52	1.05	1.03
C-70-100	6.0	0.24	0.63	0.23	0.59	1.04	1.07

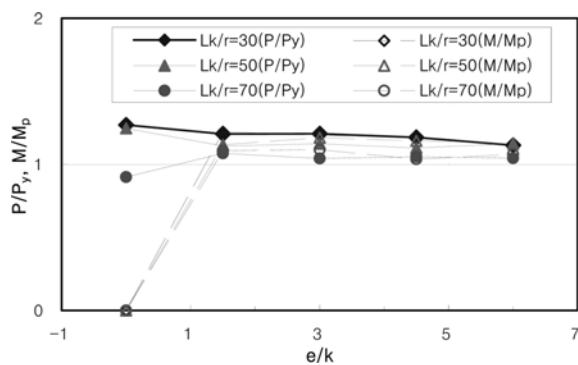


Fig. 10 Comparison of the test results and the analysis results

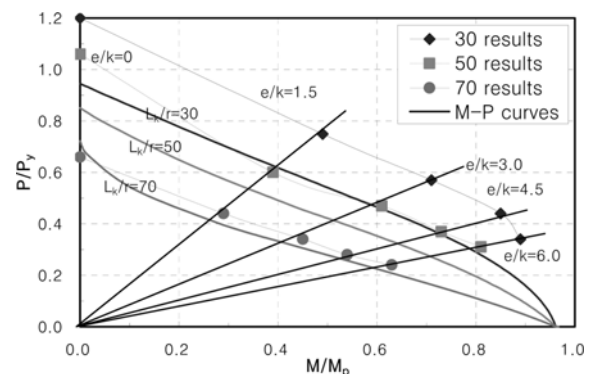


Fig. 11 M-P interaction curve

4.3 Comparison of the test results and the results of the analysis

The eccentrically compressed column was the member with a moment and an axial compressive force at the same time. The moment operated at this time occurred due to the eccentricity or the horizontal load that was directly operated with the member. In this case, the moment was mainly operated as a major buckling factor in the eccentric column and not as the axial direction compressive force.

The test results and the analysis results are compared in Table 5. Fig. 10, on the other hand, describes the values that divided the experimental values by the theoretical values based on the eccentric ratio.

The test results generally showed 4-27% higher moments and axial forces compared to the

analytical results. In the test particle with a slenderness ratio of 70 and an eccentric ratio of 0, however, 9% lower values appeared. Nevertheless, as seen in Fig. 10, as the slenderness ratio increased, the test results approached the theoretical values, such that there is a possibility that the test results with slenderness ratios of over 70 could have lower values than the analysis results.

There is a possibility that the buckling coefficient or the stress reduction coefficient that considers the slenderness ratio and that were applied in the theoretical analysis could be applied differently in the stainless steel square hollow section.

Fig. 10 shows the curve of the correlation between the moment and the axial force of the eccentric column, considering the slenderness effect, using the 0.1% offset stress of the stub-column, as well as the test results of each test particle that made the results dimensionless due to the yield stress of the stub-column and the full-plastic moment of the test particle.

Fig. 11 shows the M - P correlation curve of the slenderness ratios of 30, 50, and 70 based on the analysis results, as well as the test results of each test particle of the columns based on the slenderness ratios of 30, 50, and 70. As the slenderness ratio of the test particle increased, the test results approached the M - P correlation curve of the analysis results.

5. Conclusions

- (1) The tensile stress of the coupon test particle of the stainless steel square hollow section was 831 N/mm^2 ; the strain intensity at the maximum tensile stress was 0.504; the average offset stress at 0.1% of the yield stress was 386 N/mm^2 ; the average offset stress at 0.2% of the yield stress was 420 N/mm^2 , higher than the standard stress; and the elongation ratio was 51% with very high elongation ability. The maximum average stress by stub-column test was 406 N/mm^2 ; its strain intensity at the maximum stress was 0.0052, the 0.1% offset average yield stress was 327 N/mm^2 and the yield ratio was 0.81; and the 0.2% offset average yield stress was 389 N/mm^2 ; and the yield ratio was 0.93.
- (2) The maximum stress of the column was 393 N/mm^2 appeared in the C-30-0 test particle with 30 of slenderness ratio and 0 of eccentric ratio, and the test particle C-70-10.0, with 70 of slenderness ratio and 6.0 of eccentric ratio showed the lowest maximum stress of 79 N/mm^2 . As the slenderness ratio and eccentric ratio increased, the phenomenon of the reduction of stress was clearly observed. Also, the local buckling was occurred at 97.53% of the maximum stress.
- (3) In the relationship of the buckling stress with displacement, it was found that, as eccentric ratio at each slenderness ratio increases, the buckling stress decreases, and the displacement increase. On the other hand, as the slenderness ratio increases, axial displacement decreases but horizontal displacement increases. For the decreasing width of the axial displacements, it decreased to 88.92% on average in the test particle with a slenderness ratio of 50, and to 70.30% in the test particle with a slenderness ratio of 70 on the average, based on the test particle with a slenderness ratio of 30. While, the increasing width of the horizontal displacements increased to 147% in the test particle with a slenderness ratio of 50, and to 188% in the test particle with a slenderness ratio of 70 on the average, based on the test particle with a slenderness ratio of 30.
- (4) In the relationship between the moment and rotational angle, the moment and rotational angle based on the increase of eccentric ratio, was between 1.48-2.96 times than those when the

eccentric ratio 1.5. While the moment based on the increase of the slenderness ratio decrease to between 0.59-0.91 times, but the rotational angle increased to 1.57-2.27 times. It is considered that the increase of the end moment according to the increase of the eccentric ratio and the increase of the end rotational angle based on the increase of the slenderness ratio largely affect to the buckling of the column.

- (5) Comparing the test results with the analytical results showed that the results were satisfactory. However, since the test results approached the values of the analytical results as the slenderness ratio increased, the results of the test with a slenderness ratio of over 70 could be lower than the analytical results. This may show that the buckling coefficient or the stress reduction coefficient, which considers the slenderness ratio and which was applied in the theoretical analysis, could be applied differently to the stainless steel square hollow sections. This should be validated through further studies.

References

- AISC (2001), "Manual of steel construction: Load and resistance factor design".
- AISC LRFD (1991), "Cold-formed steel design".
- American Society of Civil Engineering (ASCE) (2003), "Specification for the design of cold-formed stainless steel structural members", SEI/ASCE-8, ASCE, Reston, Va.
- Architectural Institute of Korea (1998), "Criteria for the design and construction of steel structures".
- Architectural Institute of Korea (1998), "Criteria for the design of the compass status of steel construction".
- Bleich, F. (1952), *Buckling Strength of Metal Structures*. McGraw-Hill, New York.
- Chen, W.F. and Atsuta, T. (1976), *Theory of Beam Columns*. McGraw-Hill, Inc.
- EUROCODE No. 3 (1992), "Design of steel structures", Commission of the European Communities.
- Gardner, L. and Nethercot, D.A. (2004a), "Experiments on stainless steel hollow sections, Part 1: Material and cross-sectional behavior", *J. Constr. Steel Res.*, **60**(9), 1291-1318.
- Gardner, L. and Nethercot, D.A. (2004b), "Experiments on stainless steel hollow sections, Part 2: Member behavior of columns and beams", *J. Constr. Steel Res.*, **60**(9), 1319-1332.
- Jang, H.J., Seo, S.Y. and Yang, Y.S. (2004), "Experimental study on the comparison of the stress of the stainless steel square hollow section and of the general structural square hollow section", *Struct. J. Architectural Institute of Korea*, **20**(6), **188**, 35-42.
- Japan Stainless Steel Association (1995), "Criteria for the design and construction of stainless steel building structures".
- Johnson, John E. and Salmon, Charles G. (1996), *Steel Structures Design and Behavior*, 4th Edition, Harper Collins.
- Johnson, A.L. and Winter, G. (1996), "Behavior of stainless steel columns and beams", *J. Struct. Div.*, ASCE, **92**(5), 97-118.
- Kim, K.S., Yang, Y.S., Seo, S.Y. and Seo, J.H. (1995), "A study on the structural properties of cold-formed tubular members subjected to axial force and bending moment", *J. Architectural Institute of Korea*, **11**(6), 80, 111-124.
- Moon, T.S., Lee, M.J., Ahn, H.J. and Jang, S.K. (1992), "Experimental study on the buckling stress of the eccentrically compressed steel square hollow section", *J. Architectural Institute of Korea*, **8**(6), **44**, 175-182.